

Supplementary Information

Electro-driven direct lithium extraction from geothermal brines to generate battery-grade lithium hydroxide

Lingchen Kong¹, Gangbin Yan², Kejia Hu¹, Yongchang Yu¹, Nicole Conte³, Kevin R. Mckenzie Jr³, Michael J. Wagner³, Stephen G. Boyes³, Hanning Chen^{4*}, Chong Liu^{2*}, and Xitong Liu^{1*}

*¹Department of Civil and Environmental Engineering, The George Washington University,
Washington, D.C. 20052, United States*

*²Pritzker School of Molecular Engineering, University of Chicago, Chicago, IL 60637, United
States*

*³Department of Chemistry, The George Washington University, Washington, D.C. 20052, United
States*

*⁴Texas Advanced Computing Center, the University of Texas at Austin, Austin, TX 78758, United
States*

Corresponding authors:

xitongliu@gwu.edu;

chongliu@uchicago.edu

hanning.chen@austin.utexas.edu

Table of Contents

Fig. S1. Schematics showing the water stability window marked by H ₂ and O ₂ evolution reactions in geothermal brine. (Ewe indicates working electrode potential)	3
Fig. S2. CV curve of FePO ₄ in 1 M lithium chloride aqueous solution at a 1 mV/s scan rate. (Ewe indicates working electrode potential and I indicates specific current).....	4
Fig. S3. Electrochemical Impedance Spectroscopy (EIS) measurements in the cell system.	5
Fig. S4. XRD patterns of as-fabricated LiFePO ₄ and pre-delithiated FePO ₄	6
Table S1. Compositions of geothermal brines used in this study.	7
Fig. S5. Specific capacity vs. Ewe curve by feeding DI water and 5 mM LiCl for Li release. (Ewe indicates working electrode potential).....	8
Table S2. Atomic composition of LiFePO ₄ particle as different extraction stages.	9
Fig. S6. Module and system design of the Li extraction unit	10
Fig. S7. (a) Extraction efficiency in six series of extraction. The initial lithium concentration in the brine is 42 mM; after extraction in six cells in series, the lithium concentration remaining in the brine is 6.2 mM. (b) Photos of brine before and after extraction.	11
Table S3. Calculated enthalpy change, ΔH_{rxn} , and activation energy, ΔE_{act} , for the diffusion of various cations.....	12
Table S4. Calculated shortest metal-oxygen bond length, $DM - O$ for the initial, transition and final states along the cation's migration pathway.....	13
Fig. S8. Metal element concentration percentage in the purification process.....	14
Table S5. Other parameters used for the techno-economic assessment.....	15
Table S6. Parameters for fresh water consumption calculations.....	16
Fig. S9. pH values from the effluent in dilute-in channel along time.	17
Table S7. Lithium selectivity over major metal elements with different direct lithium extraction technologies from brines.....	18
Fig. S10. Photo of as-fabricated LiFePO ₄ composite electrode.....	20
Fig. S11. Specific capacity vs. Ewe curve in pre-delithiation process. (Ewe indicates working electrode potential)	21
Fig. S12. 3D schematic diagram of intercalative deionization cell for lithium extraction experiment.	22

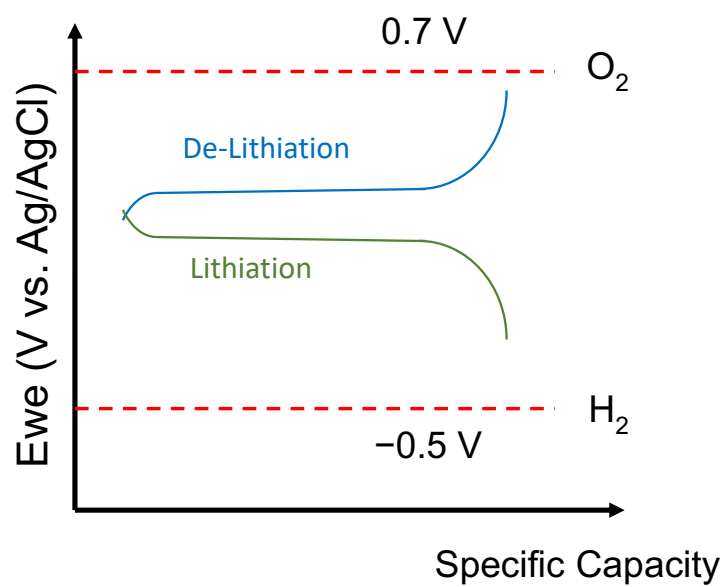


Fig. S1. Schematics showing the water stability window marked by H₂ and O₂ evolution reactions in geothermal brine. (Ewe indicates working electrode potential)

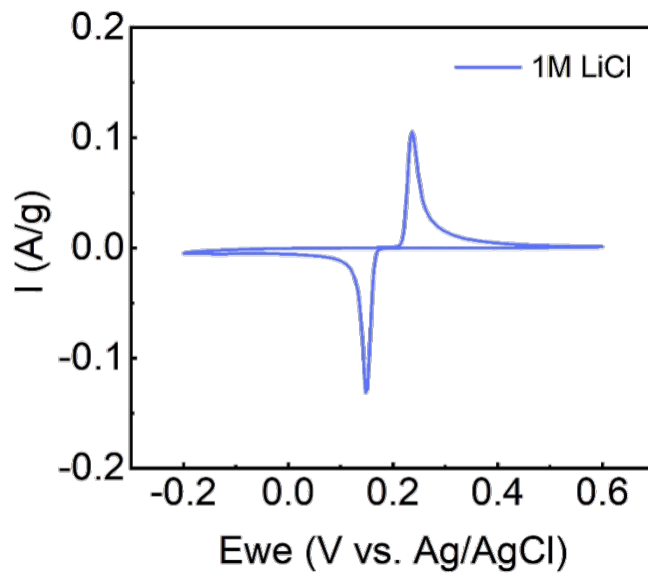


Fig. S2. CV curve of FePO₄ in 1 M lithium chloride aqueous solution at a 1 mV/s scan rate. (Ewe indicates working electrode potential and I indicates specific current). The potential is not IR corrected. Source data are provided as a Source Data file.

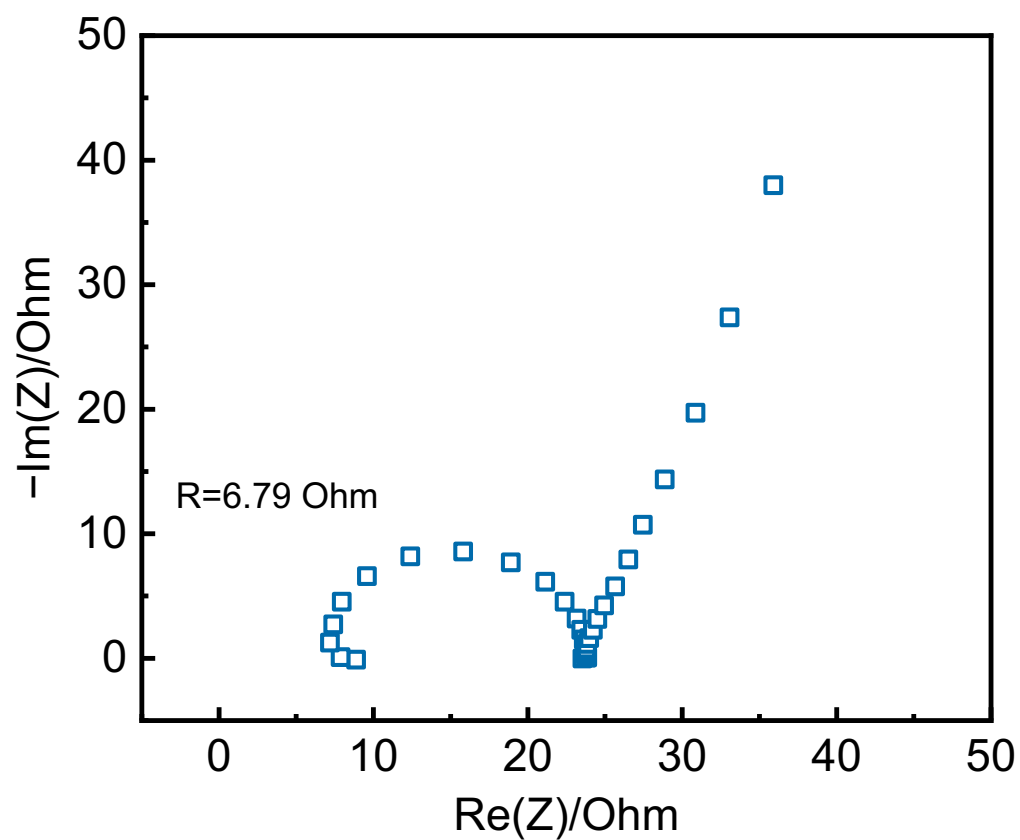


Fig. S3. Electrochemical Impedance Spectroscopy (EIS) measurements in the flow cell system. Source data are provided as a Source Data file.

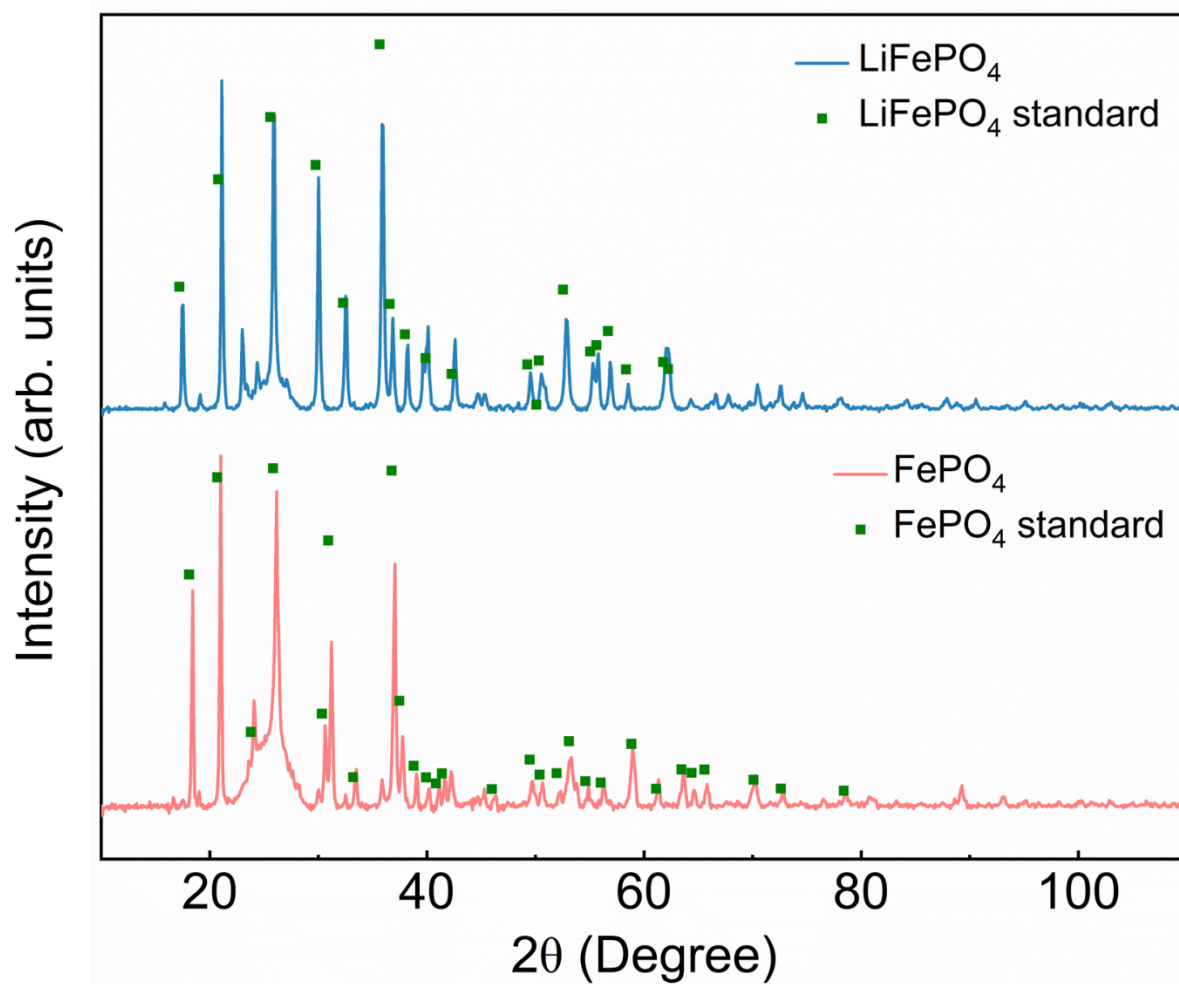


Fig. S4. XRD patterns of as-fabricated LiFePO₄ and pre-delithiated FePO₄. Source data are provided as a Source Data file.

Table S1. Compositions of geothermal brines used in this study.**a**, major components in Salton Sea wellhead geothermal brine.

Analyte	Concentration (mM)
Lithium	30
Sodium	2300
Calcium	690
Potassium	430
Magnesium	1.5

b, composition of synthetic brine based on the Simbol Feed Brine (SFB; 04/20/2011 Report of Analysis)

Analyte	Concentration (mM)
Lithium	42
Sodium	3100
Potassium	540
Calcium	1070
Iron	36
Manganese	47

c, composition of the Simbol Feed Brine (SFB; 2022 Report of Analysis)

Analyte	Concentration (mM)
Lithium	34
Sodium	2700
Calcium	940
Potassium	460
Manganese	38
Iron	30
Barium	4
Strontium	6
Lead	0.5
Copper	0.1
Magnesium	2
Aluminum	0.1
Antimony	<0.005
Arsenic	0.01
Silver	<0.01

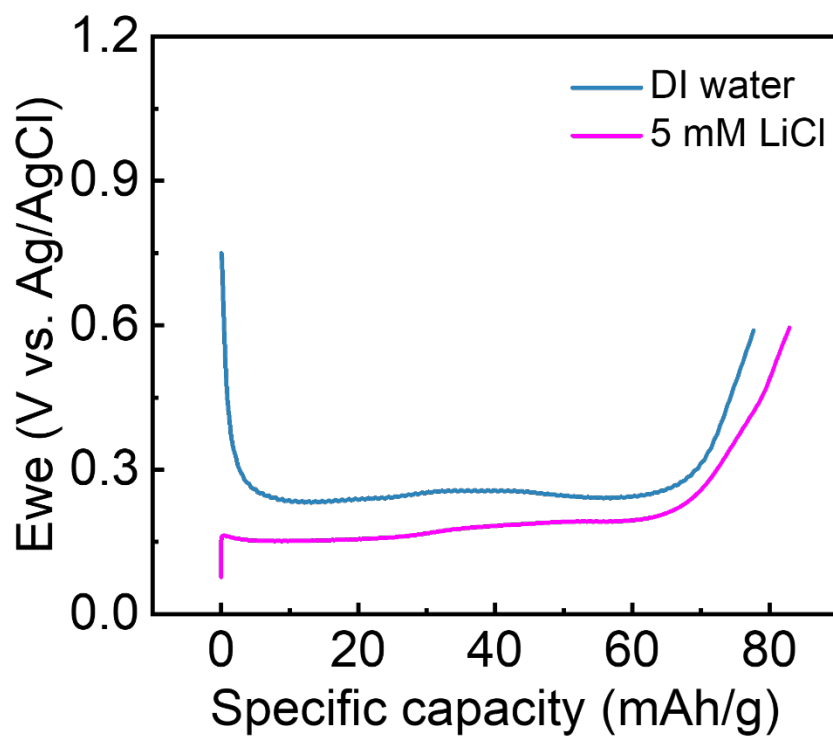


Fig. S5. Specific capacity vs. Ewe curve by feeding DI water and 5 mM LiCl for Li release. (Ewe indicates working electrode potential). The potential is not IR corrected. Source data are provided as a Source Data file.

Table S2. Atomic composition of LiFePO₄ particle as different extraction stages.

Element	Atomic percentage (%)		
	Before extraction	After extraction	After release
Na	0.0	0.2	0.0
Fe	20.1	18.7	20.5
P	17.0	17.7	16.8
O	62.8	63.4	62.6

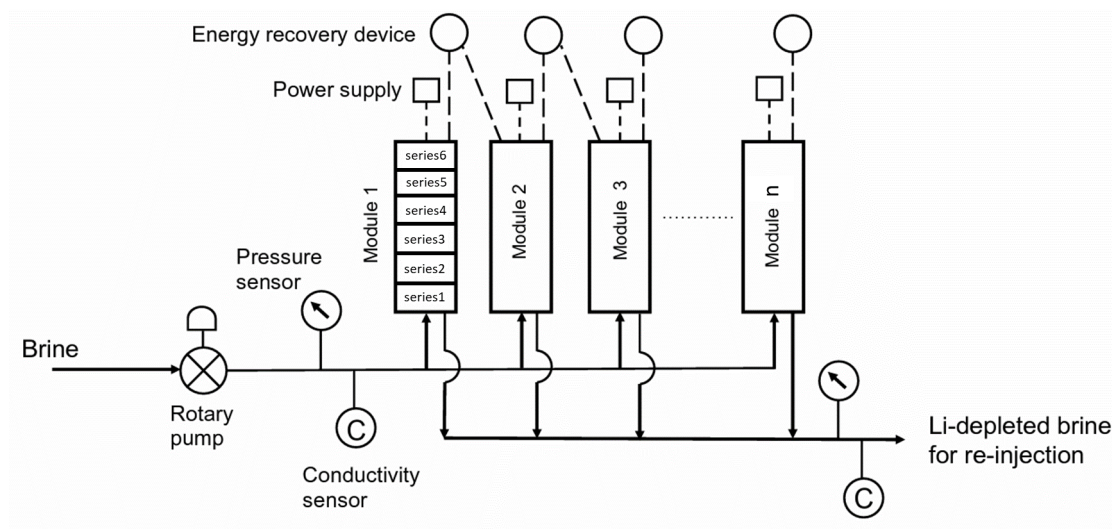


Fig. S6. Module and system design of the Li extraction unit

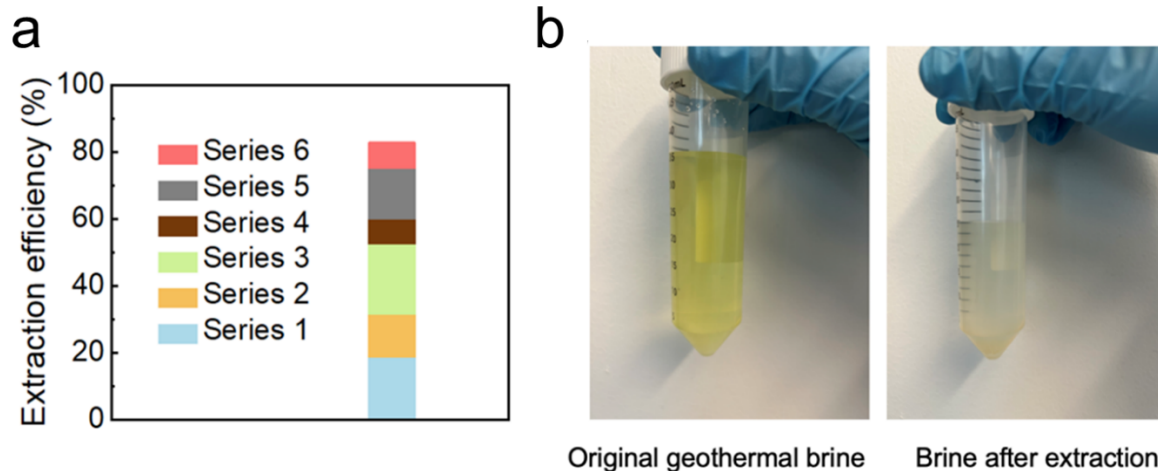


Fig. S7. (a) Extraction efficiency in six series of extraction. The initial lithium concentration in the brine is 42 mM; after extraction in six cells in series, the lithium concentration remaining in the brine is 6.2 mM. (b) Photos of brine before and after extraction. Source data are provided as a Source Data file.

Table S3. Calculated enthalpy change, ΔH_{rxn} , and activation energy, ΔE_{act} , for the diffusion of various cations.

Cation	ΔH_{rxn} (eV)	ΔE_{act} (eV)
Li ⁺	− 0.128	0.063
Na ⁺	0.082	0.404
K ⁺	N/A	N/A
Mg ²⁺	0.312	0.523
Ca ²⁺	0.663	0.942

Table S4. Calculated shortest metal-oxygen bond length, D_{M-O} for the initial, transition and final states along the cation's migration pathway.

<i>Cation</i>	$D_{M-O}^I(\text{\AA})$	$D_{M-O}^T(\text{\AA})$	$D_{M-O}^F(\text{\AA})$
Li^+	2.01	1.92	1.97
Na^+	2.18	2.03	2.13
K^+	N/A	N/A	N/A
Mg^{2+}	2.06	1.92	2.04
Ca^{2+}	2.24	2.08	2.16

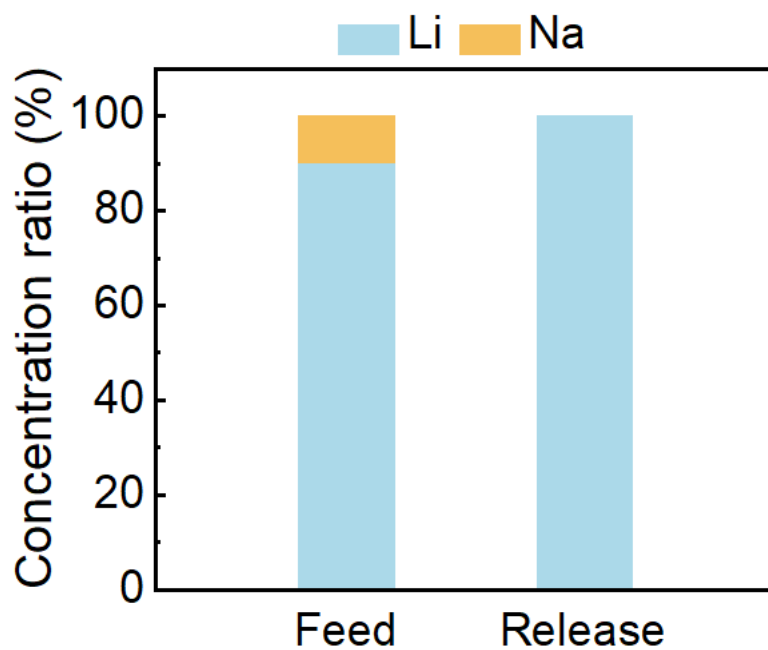


Fig. S8. Metal element concentration percentage in the purification process. Source data are provided as a Source Data file.

Table S5. Other parameters used for the techno-economic assessment

Financial parameters	Variable	Value	Unit	Source/Note
Total capital cost factor	F_{TCC}	2.0	(Total capital cost/equipment cost)	^{1,2}
Maintenance & labor factor	F_{ML}	2	% of initial total capital cost/year	^{3,4}
Chemical factor	F_C	1	% of initial total capital cost/year	³
Peripherals Factor	F_P	1.5	(Peripherals cost/membrane stack cost)	⁵
Plant Load Factor	η_{LF}	90	%	^{3,6}
Spacer cost	C_{SP}	10	\$/m ²	⁵
System parameters	Variable	Value	Unit	Source/Note
Electrode mass of active LFP	$M_{(LFP,ex\ pr)}$	65.6	mg	This work
Cycle length	τ	16	h	This work
Electrode density	ρ	0.75	g/cm ³	
Operating current	I	0.892	mA	This work
The number of treatment trains	n_{train}	1		
BMED Operating Voltage	v	2	A	Experimental Data
BMED Cross sectional area	A_{BMED}	0.25	m ²	⁷
BMED Flowrate	Q_{BMED}	0.0025	m ³ /s	⁷
The number of IEMs in a cell	n_{IEM}	4	/	This work
The number of BPMs in a cell	n_{BPM}	3	/	This work
The number of spacers in a cell	n_{SP}	8	/	This work

Table S6. Parameters for fresh water consumption calculations

Symbol	Meaning	Value	Unit
r_{wash}	The ratio of washing needed per extracted Li^+	0.15	mL/mg
Q_{wash}	Wash flowrate	0.005	mL/min
t_{wash}	Wash time	60	min
V_{wash_year}	Water volume for washing	865	m^3
$mass_{\text{LiOH_year}}$	Mass of LiOH extracted in a year	34885	kg
$mass_{\text{Li}^+_year}$	Mass of Li^+ extracted in a year	5770	kg
$mass_{\text{Li}^+_cycle}$	Mass of Li^+ extracted in a cycle	2	mg

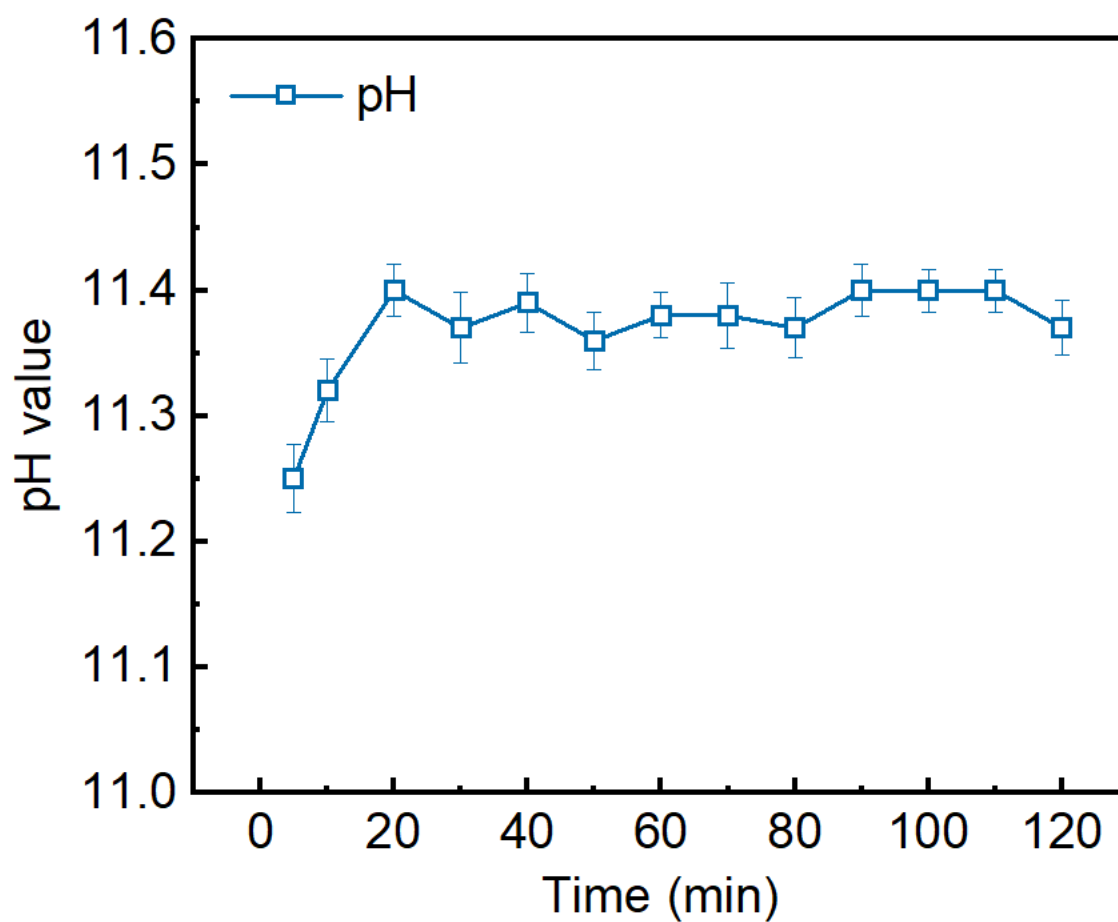


Fig. S9. pH values from the effluent in dilute-in channel along time. Source data are provided as a Source Data file.

Table S7. Lithium selectivity over major metal elements with different direct lithium extraction technologies from brines.

Ions	Molar ratio in feed	Selectivity P	Reference
Li ⁺ /Na ⁺	1:77	2.05×10³	This work
	1:10	~17	Intercalation ¹⁶
	~1:198	~12.8	Intercalation ¹⁷
	1:100	500	Intercalation ¹⁸
	~1:709	44	Adsorption ¹⁹
	1:0.8	9.8	Adsorption ²⁰
	1:1	18.2	Adsorption ²¹
	1:1	1.5	Membrane ²²
	1:1	~2.3	Membrane ²³
	1:1	~5.3	Solvent ²⁴
Li ⁺ /K ⁺	1:14.3	4.4×10³	This work
	1:10	~18	Intercalation ¹⁶
	~1:1.2	~12	Intercalation ¹⁷
	1:1	1.9	Membrane ²²
	~1:24	780	Adsorption ¹⁹
	1:1	30.6	Adsorption ²¹
	1:1	~12.3	Solvent ²⁴
Li ⁺ /Ca ²⁺	1:23	1.5×10⁴	This work
	1:10	~5	Intercalation ¹⁶
	~1:2	20	Adsorption ¹⁹

	1:1	0.9	Membrane ²²
Li ⁺ /Mg ²⁺	1:0.05	Mg undetected in released solution	This work
	1:10	~3	Intercalation ¹⁶
	1:1	57.7	Adsorption ²⁰
	1:1	15.1	Adsorption ²¹
	~1:73	40	Adsorption ¹⁹
	1:1	0.6	Membrane ²²
	1:1	~10	Membrane ²³
	~1:12	~257	Precipitation ²⁵

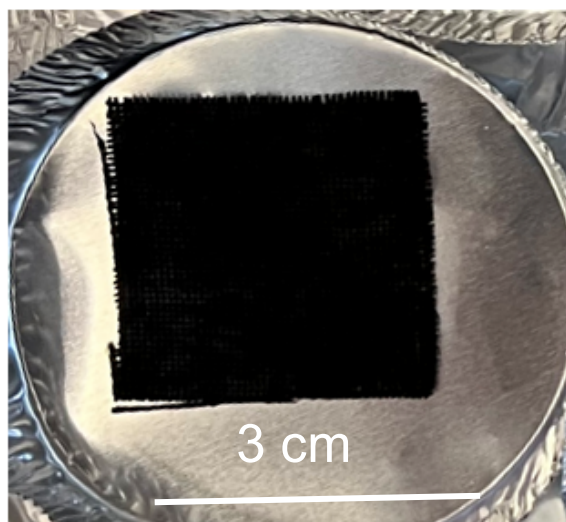


Fig. S10. Photo of as-fabricated LiFePO_4 composite electrode.

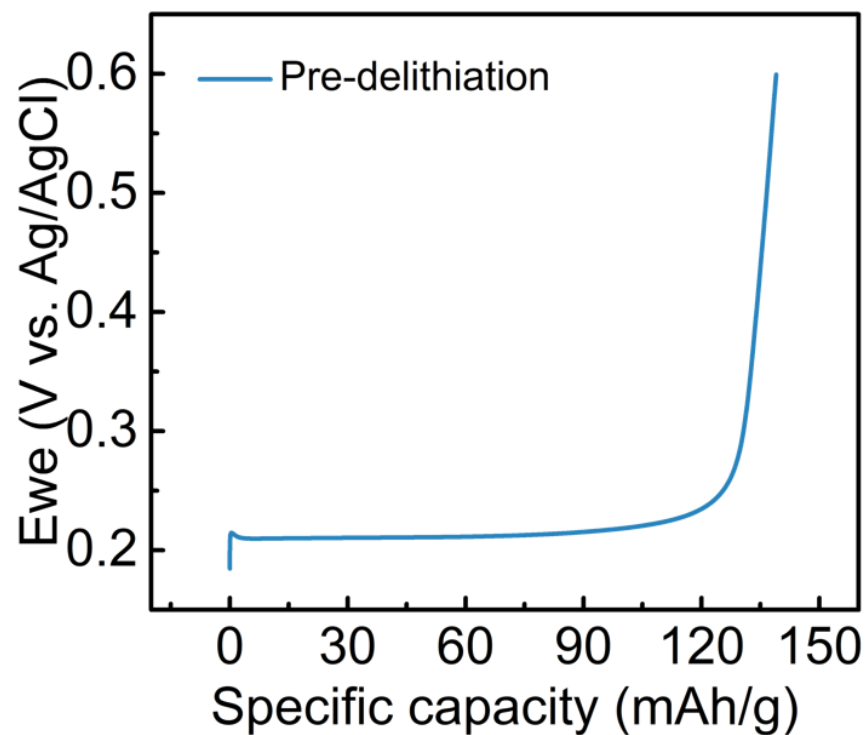


Fig. S11. Specific capacity vs. Ewe curve in pre-delithiation process. (Ewe indicates working electrode potential). The potential is not IR corrected. Source data are provided as a Source Data file.

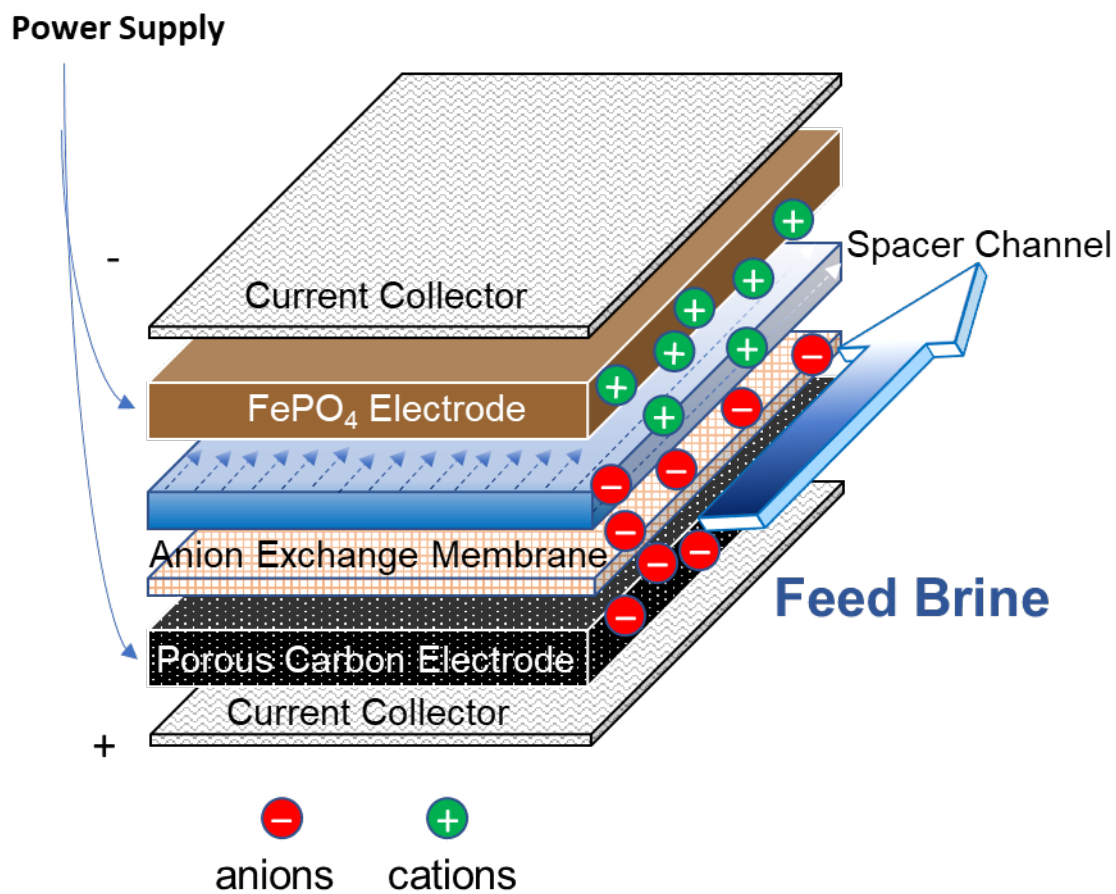


Fig. S12. 3D schematic diagram of intercalative deionization cell for lithium extraction experiment.

Supplementary References

- 1 Malek, A., Hawlader, M. N. A. & Ho, J. C. Design and economics of RO seawater desalination. *Desalination* **105**, 245-261, doi:[https://doi.org/10.1016/0011-9164\(96\)00081-1](https://doi.org/10.1016/0011-9164(96)00081-1) (1996).
- 2 Huyskens, C., Helsen, J., Groot, W. J. & de Haan, A. B. Cost evaluation of large-scale membrane capacitive deionization for biomass hydrolysate desalination. *Separation and Purification Technology* **146**, 294-300, doi:<https://doi.org/10.1016/j.seppur.2015.03.031> (2015).
- 3 Vince, F., Marechal, F., Aoustin, E. & Bréant, P. Multi-objective optimization of RO desalination plants. *Desalination* **222**, 96-118, doi:<https://doi.org/10.1016/j.desal.2007.02.064> (2008).
- 4 Park, C. *et al.* Stochastic cost estimation approach for full-scale reverse osmosis desalination plants. *Journal of Membrane Science* **364**, 52-64, doi:<https://doi.org/10.1016/j.memsci.2010.07.055> (2010).
- 5 Lei, C. *et al.* Comparative study on the production of gluconic acid by electrodialysis and bipolar membrane electrodialysis: Effects of cell configurations. *Journal of Membrane Science* **608**, 118192, doi:<https://doi.org/10.1016/j.memsci.2020.118192> (2020).
- 6 Sarai Atab, M., Smallbone, A. J. & Roskilly, A. P. An operational and economic study of a reverse osmosis desalination system for potable water and land irrigation. *Desalination* **397**, 174-184, doi:<https://doi.org/10.1016/j.desal.2016.06.020> (2016).
- 7 Culcasi, A., Gurreri, L., Cipollina, A., Tamburini, A. & Micale, G. A comprehensive multi-scale model for bipolar membrane electrodialysis (BMED). *Chemical Engineering Journal* **437**, 135317, doi:<https://doi.org/10.1016/j.ccej.2022.135317> (2022).
- 8 Poullikkas, A. Optimization algorithm for reverse osmosis desalination economics. *Desalination* **133**, 75-81, doi:[https://doi.org/10.1016/S0011-9164\(01\)00084-4](https://doi.org/10.1016/S0011-9164(01)00084-4) (2001).
- 9 Li, W.-W., Yu, H.-Q. & He, Z. Towards sustainable wastewater treatment by using microbial fuel cells-centered technologies. *Energy & Environmental Science* **7**, 911-924, doi:10.1039/C3EE43106A (2014).
- 10 Yee, R. S. L., Rozendal, R. A., Zhang, K. & Ladewig, B. P. Cost effective cation exchange membranes: A review. *Chemical Engineering Research and Design* **90**, 950-959, doi:<https://doi.org/10.1016/j.cherd.2011.10.015> (2012).
- 11 Guidelines for Preparing Economic Analyses. (U.S. Environmental Protection Agency, 2010).
- 12 Salton Sea Brine Chemistry. (U.S. Department of Energy, Geothermal Technologies Office 2021).
- 13 Strathmann, H., Grabowski, A. & Eigenberger, G. Ion-Exchange Membranes in the Chemical Process Industry. *Industrial & Engineering Chemistry Research* **52**, 10364-10379, doi:10.1021/ie4002102 (2013).
- 14 Yan, G., Wang, M., Hill, G. T., Zou, S. & Liu, C. Defining the challenges of Li extraction with olivine host: The roles of competitor and spectator ions. *Proceedings of the National Academy of Sciences* **119**, e2200751119 (2022).
- 15 Yee, R. S. L., Rozendal, R. A., Zhang, K. & Ladewig, B. P. Cost effective cation exchange membranes: A review. *Chemical Engineering Research & Design* **90**, 950-959,

- doi:10.1016/j.cherd.2011.10.015 (2012).
- 16 Lee, D.-H. *et al.* Selective lithium recovery from aqueous solution using a modified membrane capacitive deionization system. *Hydrometallurgy* **173**, 283-288, doi:<https://doi.org/10.1016/j.hydromet.2017.09.005> (2017).
 - 17 Siekierka, A., Tomaszewska, B. & Bryjak, M. Lithium capturing from geothermal water by hybrid capacitive deionization. *Desalination* **436**, 8-14, doi:<https://doi.org/10.1016/j.desal.2018.02.003> (2018).
 - 18 Pasta, M., Battistel, A. & La Mantia, F. Batteries for lithium recovery from brines. *Energy & Environmental Science* **5**, 9487-9491, doi:10.1039/C2EE22977C (2012).
 - 19 Marthi, R. & Smith, Y. R. Application and limitations of a H₂TiO₃ – Diatomaceous earth composite synthesized from titania slag as a selective lithium adsorbent. *Separation and Purification Technology* **254**, 117580, doi:<https://doi.org/10.1016/j.seppur.2020.117580> (2021).
 - 20 Kim, B., Seo, J. Y. & Chung, C.-H. Electrochemical Desalination and Recovery of Lithium from Saline Water upon Operation of a Capacitive Deionization Cell Combined with a Redox Flow Battery. *ACS ES&T Water* **1**, 1047-1054, doi:10.1021/acsestwater.1c00014 (2021).
 - 21 Li, X. *et al.* Amorphous TiO₂-Derived Large-Capacity Lithium Ion Sieve for Lithium Recovery. *Chemical Engineering & Technology* **43**, 1784-1791, doi:<https://doi.org/10.1002/ceat.201900374> (2020).
 - 22 Yu, H. *et al.* Selective lithium extraction from diluted binary solutions using metal-organic frameworks (MOF)-based membrane capacitive deionization (MCDI). *Desalination* **556**, 116569, doi:<https://doi.org/10.1016/j.desal.2023.116569> (2023).
 - 23 Warnock, S. J. *et al.* Engineering Li/Na selectivity in 12-Crown-4-functionalized polymer membranes. *Proceedings of the National Academy of Sciences* **118**, e2022197118, doi:10.1073/pnas.2022197118 (2021).
 - 24 Shi, C. *et al.* Solvent extraction of lithium from aqueous solution using non-fluorinated functionalized ionic liquids as extraction agents. *Separation and Purification Technology* **172**, 473-479, doi:<https://doi.org/10.1016/j.seppur.2016.08.034> (2017).
 - 25 Lai, X., Xiong, P. & Zhong, H. Extraction of lithium from brines with high Mg/Li ratio by the crystallization-precipitation method. *Hydrometallurgy* **192**, 105252, doi:<https://doi.org/10.1016/j.hydromet.2020.105252> (2020).